The Journal of Experimental Biology 213, 1717-1730
© 2010. Published by The Company of Biologists Ltd
doi:10.1242/jeb.036053

Mutation of the *Drosophila* vesicular GABA transporter disrupts visual figure detection

Hao Fei[1,*,†], Dawnis M. Chow[2,†], Audrey Chen[3], Rafael Romero-Calderón[1], Wei S. Ong[3], Larry C. Ackerson[1], Nigel T. Maidment[1], Julie H. Simpson[4], Mark A. Frye[2] and David E. Krantz[1,‡]

[1]Department of Psychiatry and Biobehavioral Sciences, David Geffen School of Medicine at UCLA, Los Angeles, CA 90095, USA, [2]Howard Hughes Medical Institute, Department of Integrative Biology and Physiology, UCLA, Los Angeles, CA 90095, USA, [3]Department of Neurobiology, David Geffen School of Medicine at UCLA, Los Angeles, CA 90095, USA and [4]Howard Hughes Medical Institute Janelia Farm Research Campus, Ashburn, VA 20147, USA

*Present address: Department of Nanobiomedicine, Suzhou Institute of Nano-Tech and Nano-Bionics, Suzhou Industrial Park, Suzhou, Jiangsu, 215123, China

†These authors contributed equally to this work

‡Author for correspondence (dkrantz@ucla.edu)

Accepted 2 February 2010

SUMMARY

The role of gamma amino butyric acid (GABA) release and inhibitory neurotransmission in regulating most behaviors remains unclear. The vesicular GABA transporter (VGAT) is required for the storage of GABA in synaptic vesicles and provides a potentially useful probe for inhibitory circuits. However, specific pharmacologic agents for VGAT are not available, and VGAT knockout mice are embryonically lethal, thus precluding behavioral studies. We have identified the *Drosophila* ortholog of the vesicular GABA transporter gene (which we refer to as *dVGAT*), immunocytologically mapped dVGAT protein expression in the larva and adult and characterized a *dVGAT*^{minos} mutant allele. *dVGAT* is embryonically lethal and we do not detect residual dVGAT expression, suggesting that it is either a strong hypomorph or a null. To investigate the function of VGAT and GABA signaling in adult visual flight behavior, we have selectively rescued the *dVGAT* mutant during development. We show that reduced GABA release does not compromise the active optomotor control of wide-field pattern motion. Conversely, reduced dVGAT expression disrupts normal object tracking and figure–ground discrimination. These results demonstrate that visual behaviors are segregated by the level of GABA signaling in flies, and more generally establish *dVGAT* as a model to study the contribution of GABA release to other complex behaviors.

Key words: GABA, *Drosophila*, synapse, transporter.

INTRODUCTION

Two types of neurotransmitter transporters are required for the storage and recycling of gamma amino butyric acid (GABA), and both are likely to contribute to the regulation of GABAergic neurotransmission. The plasma membrane GABA transporters (GATs1-3) remove neurotransmitter from the synaptic cleft after it is released (Kanner, 2006; Schousboe, 2000). A structurally distinct vesicular GABA transporter (VGAT) is required for its storage in synaptic vesicles (Gasnier, 2004). In mammals, VGAT is required for the storage of both GABA and glycine (McIntire et al., 1997; Wojcik et al., 2006) and is also known as the vesicular inhibitory amino acid transporter (VIAAT) (Sagne et al., 1997).

Surprisingly, it is not known how changes in VGAT/VIAAT expression or activity may affect complex behaviors potentially dependent on GABAergic neurotransmission. With the possible exception of gamma hydroxy butyrate (GHB) (Muller et al., 2002), no known drug specifically binds to or inhibits the function of VGAT/VIAAT, essentially prohibiting pharmacologic studies. The absence of available pharmacologic probes underscores the need for genetic models for in vivo analyses, but past studies of complex behavior have been relatively limited. In *C. elegans*, 25 of the 26 GABAergic neurons innervate muscle (Schuske et al., 2004) and the phenotype of the VGAT mutant *unc-47* results from deficits at the neuromuscular junction rather than the central nervous system (Brenner, 1974; McIntire et al., 1997; Schuske et al., 2004). In mice, knockout of VGAT/VIAAT is lethal and homozygous mutants die between embryonic day 18.5 and birth (Wojcik et al., 2006). GABAergic synapses in VGAT/VIAAT heterozygotes have electrophysiological properties similar to those of wild-type mice (Wojcik et al., 2006) and it remains unclear whether the heterozygotes have a detectable behavioral phenotype.

Insect visual behavior provides a potentially useful model for genetic studies of GABAergic neurotransmission and behavior. The neuroanatomy of the fly visual system has been mapped in considerable detail at both the light and ultrastructual levels (Boschek, 1971; Meinertzhagen and O'Neil, 1991; Sinakevitch and Strausfeld, 2004) and an extensive, and sophisticated battery of behavioral assays has been developed to monitor the fly's response to visual stimuli (Borst and Haag, 2002; Egelhaaf and Borst, 1993; Heisenberg and Wolf, 1984). Application of picrotoxin suggests that GABAergic signaling is required for some aspects of motion detection in *Drosophila* (Bülthoff and Bülthoff, 1987). In larger flies, both behavioral and electrophysiological assays have been used to analyze the function of one GABAergic cell type in the lobula plate proposed to be involved in figure detection (Egelhaaf et al., 1993; Warzecha et al., 1993). However, the functions of GABA release from the other ~1500 GABAergic cells in the fly optic ganglia (Buchner et al., 1988) are not known.

To help elucidate the role of GABA release in the function of the central nervous system and complex visual behavior, we have cloned and characterized the fly ortholog of the vesicular GABA transporter, which we refer to as *dVGAT*. We show that dVGAT protein is extensively expressed throughout the fly nervous system, and that mutation of the *dVGAT* gene is lethal in the embryo. In addition, using an inducible expression system to rescue the developmental lethality of *dVGAT*, we show that a decrease in adult expression of *dVGAT* compromises visual object detection.

MATERIALS AND METHODS

cDNA isolation

CG8394 cDNA generated using RT-PCR was initially synthesized from 1 μg of mRNA extracted from heads of Oregon-R *Drosophila melanogaster* Meigen, using reverse transcriptase (Roche, Indianapolis, IN, USA) and a poly(dT) oligonucleotide as primer. Polymerase chain reactions (PCR), to amplify selected regions of *CG8394*, were carried out using a PTC-200 Peltier thermal cycler (MJ Research, Inc., Waltham, MA, USA) using 2.5 i.u. of Taq polymerase (NEB, Beverly, MA, USA), 0.5 μmol l^{-1} of each appropriate primer (Operon, Huntsville, AL, USA) and 0.2 mmol l^{-1} dNTP mixture with an annealing temperature of 55°C, and an extension time of 45 s for 35 cycles. Amplification of the coding region was performed using the forward primer 5′-CGGGGTACCCAACATGTACCCCTACGACGTCCCCGACT-ACGCCATGTCATTCATAGCCAAA-3′ containing the first 18 nucleotides of the predicted open reading frame, with an added *Kpn*I restriction site, and an upstream HA tag to facilitate later expression studies. The reverse primer 5′-GCTCTAGACTAAAA-TGGAAGACCGAT-3′ contains the last 18 nucleotides of the predicted open reading frame and an *Xba*I restriction site. The location of additional primer pairs used to amplify the 5′ (r1/u1, r1/u2, r1/u3) and 3′ untranslated sequence (f3/d1, f3/d2, f3/d3) are indicated in Fig. 1A. Oligonucleotide sequences of these primers are as follows. f3: 5′-CAACCATCTGGAATCTGG-3′; d1: 5′-GACACAGCCAAATTGATG-3′; d2: 5′-CGTACATA-CTTAGGTATAC-3′; d3: 5′-TCAACTGGAGATGATGTC-3′; r1: 5′-ATAGCAGCAGATGTGTGC-3′; u1: 5′-CCATGTGAC-GACAGTAGT-3′; u2: 5′-AGTTCCATCAGGTTGGAG-3′; u3: 5′-ATGCTCTTCGAGCAGCAG-3′.

S2 cells

For expression in S2 cells, cDNA representing the *dVGAT* coding sequence was subcloned into the vector pMT/V5-His A (Invitrogen, Carlsbad, CA, USA). S2 cells were cultured as described previously (Romero-Calderón et al., 2007) and transfected using FuGENE 6 (Roche, Indianapolis, IN, USA) as per the manufacturer's instructions.

Construction of transgenes

For construction of pUAS-CG8394, RNA was isolated from wild-type adults, reverse transcribed, and the CG8394 cDNA amplified by PCR with the forward primer: 5′-TTGCGGCCGCGGCCGT-TAGTAGCCAGC-3′ and the reverse primer: 5′-GCTCTA-GAGCCCAAATGAGTCGAGTATC-3′. The resulting 1725 bp fragment was Topo cloned and digested with *Not*I and *Xba*I for insertion into pUAS, and the clones verified by sequencing. dVGAT-GAL4 was constructed by isolating genomic DNA from wild-type flies, amplifying the 6899 bp region upstream of the *CG8394* ATG by PCR with the following primers: forward 5′-TTGCGGCC-GCGGAGAGCCACGGCAGATGCCTCTTCG-3′; reverse 5′-GGGGTACCGATGCTGGCTACTAACGGCCCTGATG-3′, Topo cloning, digestion with *Not*I and *Kpn*I and insertion into the vector pPTGAL (Sharma et al., 2002). Transgenic flies were obtained by injecting w^{1118} flies carrying a stable transposase source. Three independent insertions on the X, II and III chromosomes were obtained for both the UAS and GAL4 lines. Two insertions of the GAL4 construct (on chromosomes II and III) and one insertion of the UAS construct (on chromosome III) were used for the experiments described here.

Fly husbandry

Drosophila were cultured on standard cornmeal medium at 25°C except as noted below. The following fly lines were obtained from the Bloomington *Drosophila* Stock Center at Indiana University (Bloomington, IN, USA): *tub-GAL80*^{ts} (stock 7018) and the *minos* insertion line *CG8394*^{MB01219} (designated in the text as *dVGAT*^{minos1}), maintained over the *CyO* balancer chromosome. The insertion site of the *minos* element in *dVGAT* is indicated in Fig. 1A,C. Prior to phenotypic analysis, *dVGAT*^{minos1} was outcrossed for five generations in the wild-type strain w^{1118} (Canton S background). To obtain *dVGAT* knockdown animals for behavioral experiments, flies were allowed to mate and lay eggs in vials containing standard food at 30°C for up to 5 days, and the vials observed twice daily for evidence of pupation. Under these conditions, the time from the beginning of pupation to eclosion was ~80 h, and flies were moved to 18°C at ~40 h or 50% completion. Flies that eclosed the day after transfer to 18°C were discarded, and those that eclosed on subsequent days were collected and aged for 5–7 days at 18°C. Female flies were used for all behavioral experiments.

Antibody generation

The rabbit anti-dVGAT antibody was raised against a C-terminal peptide (–CDSGNALINAFEIGLPF) conjugated to KLH protein by Covance Research Products (Princeton, NJ, USA). A cysteine residue was introduced to the N-terminus of the peptide to facilitate covalent conjugation to KLH protein and an affinity purification matrix (see below). The crude antisera were first tested against fly brain homogenates using western blots. Antisera with higher titer were used for further affinity purification: 1 mg of sulfhydryl-containing peptide was conjugated to 3 ml UltraLink Iodoacetyl Gel (Pierce, Rockford, IL, USA) according to the manufacturer's instructions. Briefly, 5 ml antiserum was first diluted with 5 ml of PBS (150 mmol l^{-1} NaCl, 10 mmol l^{-1} $NaPO_4$, 5 mmol l^{-1} KCl, pH 7.4) containing 0.2% Triton X-100 and then loaded onto a PBS-equilibrated affinity column. The column was then washed with PBS and the bound antibody was eluted by applying glycine buffer (100 mmol l^{-1}, pH 2.5). Collected fractions were neutralized by adding one-tenth volume of 1 mol l^{-1} Tris, pH 7.5. Purified antibody was used at a dilution of 1:1000 for western blots and either 1:200 or 1:400 for immunofluorescence labeling experiments as indicated below.

Biochemical fractionation

Glycerol gradient fractionations were performed as described previously (Daniels et al., 2004). Samples from each fraction were subjected to SDS-PAGE and probed on western blots using primary antibodies to dVGAT (1:1000) and *Drosophila* Cysteine string protein (CSP, 1:1000; Developmental Studies Hybridoma Bank at University of Iowa), followed by the appropriate HRP-conjugated secondary antibody (Amersham Biosciences, Arlington Heights, IL, USA) and a chemiluminescent substrate (SuperSignal West Pico, Pierce, Rockford, IL, USA).

Immunolabeling

Embryos were aged for 15–18 h, dechorinated in 50% bleach, then devitellinized and fixed in 50% heptane, 2% paraformaldehyde, PBS for 40 min at ambient temperature, followed by washes in ethanol and PBS containing 0.2% Triton X-100 (PBST). Embryos were incubated for 30 min at ambient temperature in PBST containing 10% fetal bovine serum and in anti-dVGAT (1:200) overnight at 4°C. Secondary antibody (anti-rabbit Alexa Fluor 555; Molecular Probes/Invitrogen, Eugene, OR, USA) was used at 1:1000, with an overnight incubation at 4°C to improve permeabilization. After washing, embryos were mounted on coverslips using Aqua Poly/Mount (Polysciences, Warrington, PA, USA).

For co-labeling of dVGAT and GABA, the larval brain and ventral nerve cord was dissected in PBS and fixed in PBS containing 25% glyceraldehyde, 4% paraformaldehyde for 2 h at ambient temperature. For all other immunolabelings, larval and adult fly brains were dissected in PBS and fixed in 4% paraformaldehyde (in PBS) for 2 h at ambient temperature. Brains were then washed in PBST and blocked for 1 h at ambient temperature in PBST containing 5% fetal bovine serum. Primary anti-dVGAT was diluted 1:400 in PBST and incubated overnight at 4°C. Additional primary antibodies included 1:500 guinea pig anti-GABA (Abcam, Cambridge, MA, USA), 1:125 rabbit anti-horseradish peroxidase (HRP; Sigma-Aldrich, St Louis, MO, USA), 1:25 mouse anti-*Drosophila* Cysteine string protein (mAb 1G12; Developmental Studies Hybridoma Bank, University of Iowa), and 1:10 mouse anti-Bruchpilot (mAb nc82; Developmental Studies Hybridoma Bank, University of Iowa). Secondary antibodies included 1:2000 dilutions of one or more of the following: anti-rabbit Alexa Fluor 488 or 555, anti-mouse Alexa Fluor 488 or 555 or anti-guinea pig Cy3 (Jackson ImmunoResearch, West Grove, PA, USA). After washing, brains were equilibrated in 70% glycerol in PBS and mounted on coverslips using ProLong Antifade (Molecular Probes/Invitrogen, Eugene, OR, USA). To label adult thoracic ganglia, we a used a protocol posted by Richard Carthew on the website http://www.biochem.northwestern.edu/carthew/manual/Wholeflystain.html. Briefly, whole adult flies were incubated with gentle agitation for 20 min at ambient temperature in 12.5% formaldehyde, 50 mmol l^{-1} NaP_i pH 6.8, 50% octane, then rinsed in octane and dissected in PBS to remove the dorsal half of the thorax. The ventral half of the thorax was then post-fixed for 90 min at 0°C in 4% formaldehyde, 100 mmol l^{-1} NaP_i pH 6.8, and washed twice in PBS. The thoracic ganglion was removed in PBS and immunolabeled as described above for adult brains, except that anti-rabbit Cy3 (Jackson ImmunoResearch) was used as a secondary antibody.

HPLC

Analysis of GABA content was performed by HPLC-fluorescence detection of ortho-phthalaldehyde (OPA)-derived samples as previously described (Murphy et al., 1999). Briefly, four heads of female flies were manually homogenized (~10 strokes) in 50 µl of chilled 0.1 mol l^{-1} perchloric acid (PCA), 0.1% EDTA buffer using a glass-on-glass micro tissue grinder (Kontes Art. No. 885470-0000, Vineland, NJ, USA) on ice. An additional 25 µl of 0.1 mol l^{-1} PCA, 0.1% EDTA buffer was used to rinse the pestles and collect the homogenate. The tubes were briefly microcentrifuged (1 min, 13,200 r.p.m.) to remove large debris and the eluate applied to an Ultrafree-MC (Millipore cat. no. UFC30GV00) centrifugal filter unit. The filtrate was frozen and stored at –80°C until pre-column OPA derivatization and injection onto a reversed-phase column followed by elution of the GABA–OPA adduct with an organic gradient.

Behavioral analysis

An electronic LED flight simulator presented visual cues and tracked the wing motions of tethered flies. The difference between the left and right wing beat amplitude closes a feedback loop with the rotational velocity of the digital display, allowing flies active control over the visual panorama in a manner consistent with free flight. The digital flight arena has been described previously (Duistermars et al., 2007). Briefly, the arena was composed of 48, 8×8 LED panels arranged in a cylinder. A cold-anesthetized fly was tethered to a steel pin and suspended in the center of the arena. An infrared diode cast a shadow of the beating wings onto a two-part optical sensor, which encoded the frequency and amplitude of each wing stroke for the right and left wings independently. For each wing beat, the stroke amplitude and frequency were digitized at 500 Hz and stored for later analysis.

Inducible *dVGAT* knockdown flies and constitutively rescued control flies were shifted in parallel from 30°C to 18°C as brown pupae and subjected to the same protocols. For all treatments, adult female flies were tested 5–7 days after eclosion. After tethering under cold anesthesia, flies were allowed 1 h to recover. Only data from animals that flew consistently over the entire 3 min trial were included in the analysis. A visual object was composed of a vertical bar subtending 15×120 deg. (width × height) on the retina and the wide-field panorama was composed of a random array of 30×30 deg. dark blocks (random checkerboard) subtending 360×120 deg. on the retina. For the combined figure–ground pattern, the object always moved opposite the random checkerboard background with equal angular velocity.

Under closed-loop feedback, motion of the visual panorama is fully guided by the steering kinematics of the fly's wings (see Results). Flies make constant adjustments to their flight heading, which moves the panorama and provides rich visual feedback indicating self motion. However, if an animal is somehow compromised in its ability to steer, then the panorama will not move, resulting in near-zero angular velocity. This result could erroneously appear to represent robust optomotor stabilization. To control for this potential pitfall, we further challenged flies by adding a sine-wave bias to the feedback loop. The biased signal was a sinusoid frequency=1 Hz, amplitude=±15 deg. Under these 'biased closed-loop' conditions, flies can only maintain active control over the visual display by steering against the imposed bias.

Each fly was presented with the bar in closed-loop for 20 s and in biased closed-loop for 20 s. For each assay we analyzed 10–15 experimental (knockdown; see text) and 10–15 control (constitutive rescue) flies.

RESULTS

CG8394 encodes a *Drosophila* ortholog of VGAT

The *Drosophila* genome contains a single predicted gene (*CG8394*) similar to previously identified orthologs of VGAT (McIntire et al., 1997; Sagne et al., 1997) (Fig. 1A). No other sequences in the public database show comparably high similarity to mammalian VGAT orthologs (not shown). At the time that we began our analysis of *CG8394*, cDNA clones were not available, and, until recently, the clone currently available from the Berkeley *Drosophila* Genome Project (BDGP IP12576, http://flybase.net/reports/FBcl0303860.html) appeared to be truncated at the 3′ end (see below). To identify a full-length cDNA representing *CG8394*, we used reverse transcription and PCR (RT-PCR) with primers based on the predicted sequence of *CG8394* (BDGP; http://flybase.bio.indiana.edu/reports/FBgn0033911.html). RT-PCR using primers that bracket the predicted start and stop codons (the large open reading frame)

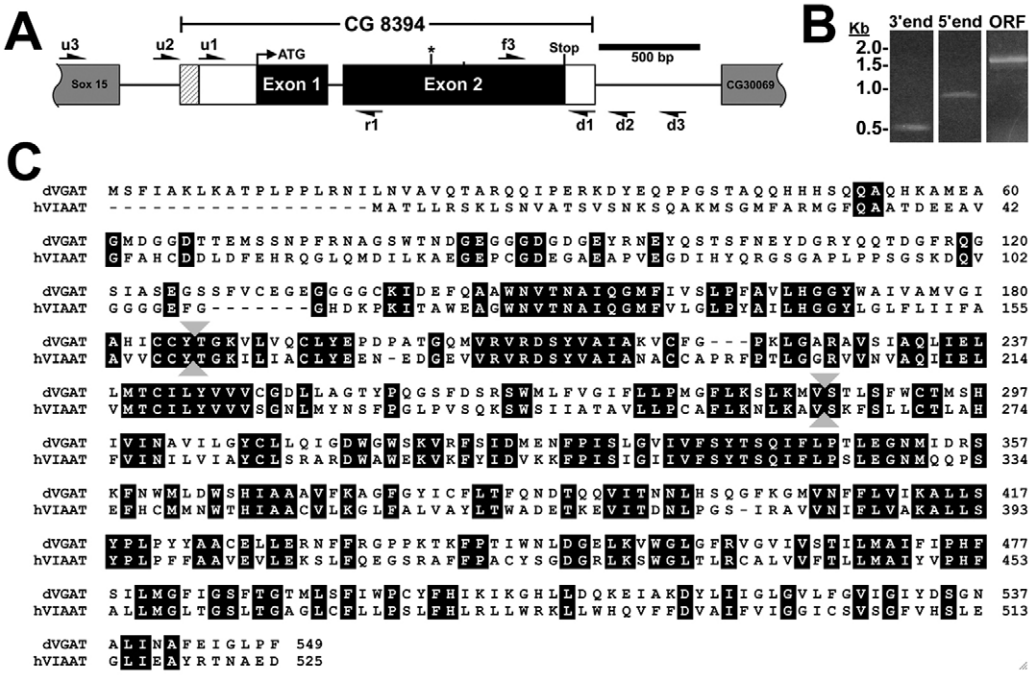

Fig. 1. Cloning of the *Drosophila* vesicular γ-amino butyric acid (GABA) transporter (CG8394). (A) *CG8394/dVGAT* is between *CG30069* and *Sox15* on the right arm of chromosome II. Exons are shown as boxes, with coding sequence in black and untranslated sequence in white. Introns are indicated as black lines. The 5′ extent of the BDGP clone IP12576 is indicated with hatching. Arrows indicate primers used for RT-PCR to define the 5′ and 3′ extent of the cDNA and an asterisk indicates the insertion site of the minos element. (B) The approximate 3′ and 5′ extent of *CG8394*. Untranslated regions (UTRs) were mapped by selectively amplifying *CG8394* products using primer pairs f3/d1 (3′ end) and r1/u1 (5′ end) but not more distal primers (see Results). RT-PCR to amplify the coding sequence shows a 1.7 kb product (ORF). Size markers are shown on the left, in kilobases. (C) The predicted amino acid sequence of dVGAT is shown aligned with human VIAAT/VGAT. Identities are highlighted. Identity at the amino acid level is 44%; for comparison dVGLUT shows 41% identity with human VGLUT orthologs (Daniels et al., 2004). Gray arrowheads between amino acids 118 and 119, and between 286 and 287 indicate the site of the mRNA splice junction and the insertion site of the *minos* element, respectively.

yields a single 1.7 kb product (Fig. 1B, open reading frame, ORF). Comparison of cDNA and genomic sequence confirms the excision of a single intron within the coding sequence as shown in Fig. 1A.

To determine the 5′ and 3′ extent of the mRNA, we initially attempted rapid amplification of cDNA ends (RACE) using internal primers within the coding sequence of *CG8394*. Sequencing revealed that all products were truncated relative to the sequence of known VGAT orthologs (not shown). As an alternative strategy to identify additional 5′ and 3′ mRNA, we performed RT-PCR using a series of primers between the predicted CG8394 open reading frame and its neighboring genes (see Fig. 1A, primers d1-3 and u1-3). We obtained products of the appropriate size using the 5′ primer u1 (~200 bp upstream of the predicted start codon) and a 3′ primer in the *dVGAT* coding region (Fig. 1A, r1). We also obtained a product using the 3′ primer d1 which is 100 bp downstream of the predicted stop codon, and a 5′ primer (f3) in the coding region of *dVGAT*. By contrast, we did not obtain products using the primers farther upstream or downstream form the ORF (d2, d3, u2, u3; data not shown). Furthermore, multiple stop codons were present in all three reading frames of the 5′ region upstream of the predicted initiating methionine. It is therefore likely that we have identified the full extent of the CG8394 ORF. The alignment of CG8394 and the human ortholog of VGAT are shown in Fig. 1C. Identity at the amino acid level is 44% and identical residues are highlighted. For comparison, DVGLUT shows 41% identity with human VGLUTs (Daniels et al., 2004). Based on the similarity between *CG8394* and other VGAT orthologs, as well as the expression data we show below, we refer to the *CG8394* gene as *Drosophila* VGAT (*dVGAT*).

The coding region of CG8394 together with the additional 5′ and 3′ untranslated regions amplified using RT-PCR make up a total of ~2 kb. We detect a single band of ~2–3 kb representing *CG8394* on northern blots (Romero-Calderón et al., 2007). The sequence originally reported by BDGP for clone IP12576 suggested that it was missing the last 600 bp of coding sequence (it has now been corrected). Up to the site of the previous truncation (and now throughout the entire coding region), the predicted amino acid sequence is identical to that shown in Fig. 1A. In addition, the 5′ end of the BDGP cDNA IP12576 includes 200 bp between the primers u1 and u2 shown in Fig. 1A; the 5′ extent of the BDGP cDNA is ~20 bp downstream from primer u2, which failed to give an RT-PCR product. Together, these data suggest that the 5′ extent of the transcript is ~220 bp upstream of the predicted start codon. The extent of the additional sequence is shown in Fig. 1A as the hatched area of exon 1.

dVGAT protein localizes to synaptic vesicles

To facilitate an analysis of dVGAT protein localization *in vivo*, we developed an antibody directed against the last 16 amino acids of the C-terminus (see Materials and Methods). The antibody to dVGAT, but not preimmune serum (data not shown) recognizes a single band on western blots (Fig. 2A) migrating at a molecular mass of 60 kDa, consistent with the predicted size of the protein (60.8 kDa). To help determine the subcellular localization of dVGAT, we first expressed the dVGAT cDNA in cultured S2 cells. We observed a punctate pattern consistent with its localization to intracellular, membranous compartments (Fig. 2B), and also

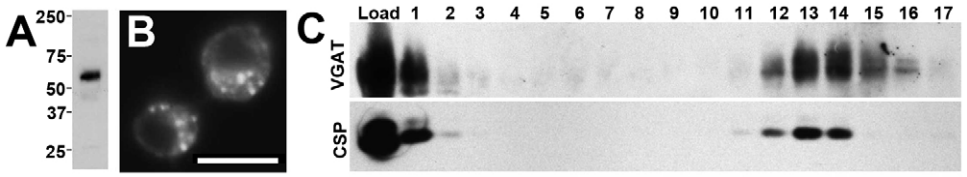

Fig. 2. Expression of dVGAT protein. (A) Western blots of head homogenates probed with an antibody to dVGAT show a single major band. Standards (in kDa) are indicated on the left. (B) Cultured *Drosophila* S2 cells expressing the *dVGAT* cDNA and labeled with the antibody to dVGAT show punctate intracellular labeling. Scale bar, 10 μm. (C) Glycerol velocity gradients show that dVGAT partially co-sediments with a marker for synaptic vesicles (CSP).

consistent with the pattern we observed for both *Drosophila* VMAT and VGLUT (Daniels et al., 2004; Greer et al., 2005).

To determine the subcellular localization of dVGAT *in vivo*, we used the anti-dVGAT antibody to probe glycerol velocity gradients, an established method of separating synaptic vesicles from other organelles (Clift-O'Grady et al., 1990; van de Goor et al., 1995). We found that dVGAT co-sediments with the synaptic vesicle marker *Drosophila* CSP (Zinsmaier et al., 1990) (Fig. 2C), similar to both DVMAT and DVGLUT (Chang et al., 2006; Daniels et al., 2004) and consistent with its predicted function as a vesicular transporter. We note that dVGAT was present in some fractions that showed relatively low levels of CSP. It is possible that in some cells, dVGAT may reside on organelles other than classically defined synaptic vesicles.

A mutant allele of *dVGAT* is lethal

To investigate the function of *dVGAT in vivo*, we characterized a lethal allele of *dVGAT* generated by the insertion of a *minos* transposable element within the second exon (Metaxakis et al., 2005) (see Fig. 1A, asterisk). To identify the developmental phase at which $dVGAT^{minos1}$ is lethal, we took advantage of the fact that *minos* elements are marked with GFP (Metaxakis et al., 2005). In ~200 embryos, we observed the expected Mendelian ratio of strongly labeled homozygotes, and less intensely labeled $dVGAT^{minos1}/CyO$ heterozygotes. None of the approximately 50 intensely fluorescently labeled homozygous embryos were observed to hatch, confirming the $dVGAT^{minos1}$ allele is embryonically lethal.

To help define the severity of the $dVGAT^{minos1}$ allele, we first attempted to use western blots to quantify embryonic dVGAT expression. dVGAT protein levels were below our limit of detection using up to 30 wild-type embryos (not shown), thus making it difficult to use western blotting to determine whether *dVGAT* mutants might express residual dVGAT protein. We therefore probed for residual protein expression using immunolabeling. We used the anti-dVGAT antibody followed by a fluorophore-conjugated secondary antibody to label embryos derived from the $dVGAT^{minos1}/CyO$ line (Fig. 3A–D) and again took advantage of the GFP tag in the *minos* insertion. In homozygous mutant embryos showing high levels of GFP expression (Fig. 3A,B), we were unable to detect any specific labeling for dVGAT (Fig. 3C,D). By contrast, in embryos showing intermediate levels of GFP expression (Fig. 3A,B), the ventral nerve cord was robustly labeled for dVGAT (Fig. 3C,D). Higher resolution, confocal images of another heterozygote showing intermediate levels of GFP expression (Fig. 3E) confirm the specific labeling for dVGAT in the ventral nerve cord (Fig. 3F). There was no specific labeling for dVGAT in a homozygote showing higher levels of GFP expression (Fig. 3H–J). Autofluorescence of the gut in all embryos can be seen in both the red (Fig. 3F,I) and green channels (Fig. 3E,H) as well as the merged images (Fig. 3G,J). These data suggest that $dVGAT^{minos1}$ is either a strong hypomorph or a null allele, although we cannot rule out the possibility that it has some residual activity. In addition, these data confirm the specificity of the dVGAT antibody.

dVGAT protein is expressed in the larval brain and ventral nerve cord

We next used the dVGAT antibody to examine the expression of dVGAT in larvae (Fig. 4). We detected at least six clusters of cell bodies in the larval central brain (Fig. 4A–C) similar to the distribution of glutamic acid decarobxylase (GAD) (Enell et al., 2007), another marker for GABAergic cells. In the nerve cord, labeled somata were found to be distributed primarily near the ventral surface in a segmental pattern (Fig. 4D,E). The more dorsal neuropil was also extensively labeled (Fig. 4D). A previously reported antibody to the dVGAT N-terminus shows a similar pattern in the neuropil, but does not detect dVGAT in cell bodies, as we show here (Enell et al., 2007). All cells expressing dVGAT in the nerve cord appear to co-label for GABA (Fig. 4F–H). These data are consistent with the notion that dVGAT is required only in cells that release GABA. By contrast, mammalian VGAT/VIAAT is required for glycine as well as GABA storage (Wojcik et al., 2006).

dVGAT is widely expressed in the adult nervous system

In the adult fly, we observed widespread, punctate labeling for dVGAT throughout the adult central brain and optic lobes (Fig. 5), consistent with previous reports using GABAergic markers in *Drosophila* and other insects (Brotz and Borst, 1996; Brotz et al., 2001; Enell et al., 2007; Harrison et al., 1996; Meyer et al., 1986; Sinakevitch et al., 2003; Sinakevitch and Strausfeld, 2004; Strausfeld et al., 1995). Labeled structures in the central brain include the subesophageal ganglion (Fig. 5A,B, SOG), antennal lobe (Fig. 5A, Al) and both the ellipsoid body (Fig. 5I) and fan-shaped body (not shown) of the central complex. dVGAT was also expressed throughout the optic ganglia. In the lamina, we observed labeled processes morphologically consistent with projections of the C2 cell type, previously proposed to contain GABA (Buchner et al., 1988; Datum et al., 1986). More recently, C3 also has been suggested to store GABA (Enell et al., 2007; Kolodziejczyk et al., 2008; Sinakevitch et al., 2003), and anti-dVGAT labeled C3-like processes in the lamina. In the medulla, tangential fibers expressed dVGAT (Fig. 5D, arrow). These may correspond to widely projecting tangential processes seen in larger flies and bees (Meyer et al., 1986; Schafer and Bicker, 1986; Sinakevitch and Strausfeld, 2004). We also observed a large number of small cell bodies in the cortical rind of the medulla (Fig. 5D, arrowhead and 5F). Centripetal projections from these cells appear to contribute to the columnar labeling for dVGAT in the outer (Fig. 5E) and perhaps the inner medulla. These may be transmedullary (Tm) cells (see Discussion).

The neuropil of both the lobula and lobula plate also labeled for dVGAT (Fig. 5B,G). Some labeling in the lobula is likely to be of the tangential processes (Meyer et al., 1986; Sinakevitch and

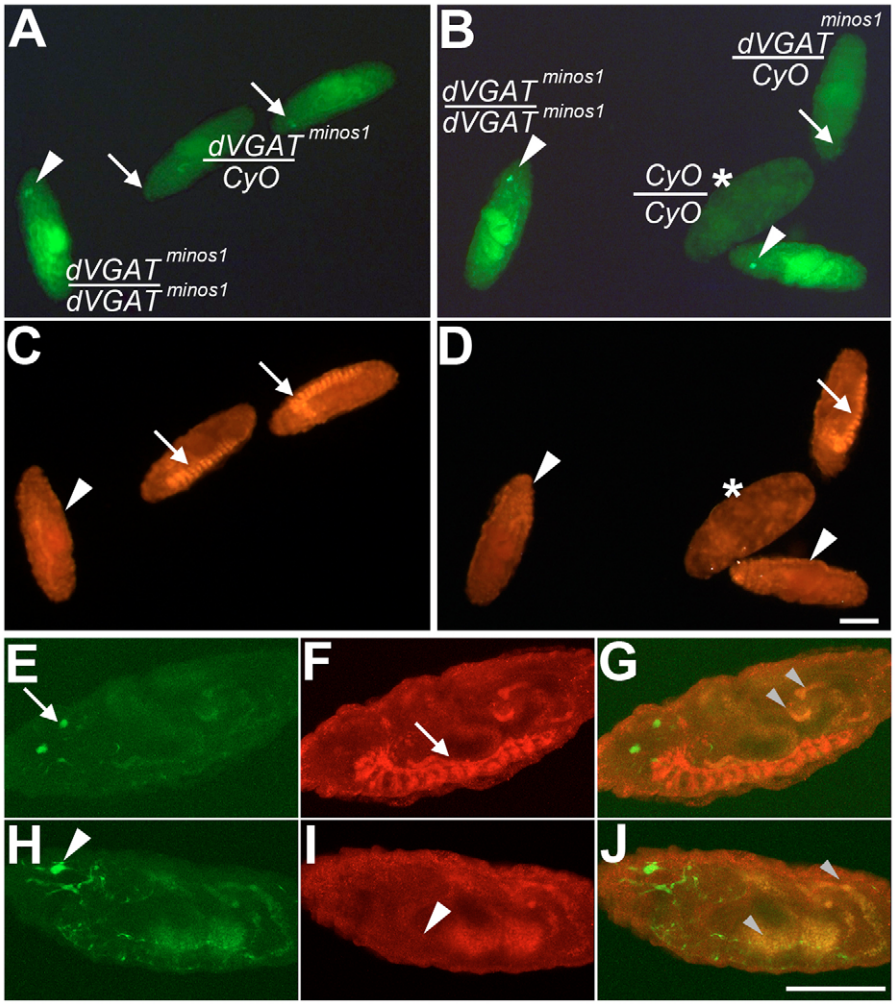

Fig. 3. A *dVGAT* mutant. Embryos were derived from $dVGAT^{minos1}$/*CyO* parents, and visualized using a standard upright (A–D) or confocal (E–J) microscope. Embryos from two separate low-power fields are shown in A,C and B,D. For all panels, anti-dVGAT, labeling is in red and endogenous fluorescence of GFP is green. Intense GFP fluorescence (A,B white arrowheads) is seen in embryos homozygous for the GFP-tagged *minos* insertion ($dVGAT^{minos1}$/$dVGAT^{minos1}$). These embryos do not show specific labeling for dVGAT in the ventral nerve cord (C,D, white arrowheads). Embryos showing less intense GFP fluorescence (A,B, white arrows) are heterozygous for the mutation ($dVGAT^{minos1}$/*CyO*) and show robust labeling for dVGAT in the nerve cord (C,D, white arrows). The remaining, malformed embryo shown in B and D (asterisk) is presumably *CyO*/*CyO*. (E–G) Confocal images of additional embryos. A $dVGAT^{minos1}$/*CyO* heterozygote (E–G) shows moderate GFP fluorescence (E, white arrow) and labeling of dVGAT in the ventral nerve cord (F, white arrow). A $dVGAT^{minos1}$/$dVGAT^{minos1}$ homozygote shows high levels of GFP fluorescence (H, arrowhead) and no specific labeling of dVGAT in the nerve cord (I, white arrowhead). As seen in the merged images (G,J), both heterozygotes and homozygotes show non-specific autofluorescence in the gut (small grey arrowheads). Scale bars, 100 μm.

Strausfeld, 2004), and in the lobula plate may be of the terminals presynaptic to tangential neurons (LPTCs; lobula plate tangential cells) that integrate retinotopic information (Hausen, 1984) (see Discussion). dVGAT is also widely expressed in the neuropil of the thoracic ganglion (Fig. 5J–L), including labeling of some nerve roots, possibly suggesting a peripheral function for GABAergic signaling.

Inducible transgenes can rescue the *dVGAT* mutant thereby allowing behavioral analyses

To allow both constitutive and inducible rescue/knockdown of $dVGAT^{minos1}$, we used the well-characterized GAL4/UAS system (Brand and Perrimon, 1993). We constructed *dVGAT-GAL4* lines containing the 6.9 kb upstream of the initiating methionine of *dVGAT*, and here used transgenes on chromosomes II and III (*dVGAT-GAL4(II)* and *dVGAT-GAL4(III)*). UAS transgenes were constructed using the predicted 1.7 kb open reading frame of *dVGAT* encoding the sequence shown in Fig. 1C; here we use an insert on chromosome III (*UAS-dVGAT(III)*). To determine the expression pattern generated by *dVGAT-GAL4* transgenes, lines were crossed to flies containing a *UAS-GFP* transgene (Fig. 6A,B). The *dVGAT-GAL4* drivers localizing to the second (Fig. 6A) and third chromosomes (Fig. 6B) showed a broad expression pattern in both the central brain and optic lobes. To determine whether the *GAL4* lines allow expression of functional dVGAT in GABAergic cells, we performed genetic rescue experiments using the $dVGAT^{minos1}$ allele. We found that $dVGAT^{minos1}$ homozygotes containing *VGAT-GAL4(III)* and *UAS-dVGAT(III)* ($dVGAT^{minos1}$; *dVGAT-GAL4(III), UAS-dVGAT(III)*) as well as *dVGAT* mutants containing *dVGAT-GAL4(II)* and *UAS-dVGAT(III)* ($dVGAT^{minos1}$, *dVGAT-GAL4(II); UAS-dVGAT(III)*) rescue the $dVGAT^{minos1}$ allele and were both viable and fertile. These observations confirm that the *UAS-dVGAT* transgene encodes a functional protein. In addition, rescue using either *dVGAT-GAL4(II)* or *dVGAT-GAL4(III)* indicates that both GAL4 transgenes are expressed at least in those GABAergic neurons required for development and survival.

We hypothesized that transient expression of dVGAT during development might rescue the embryonic lethality of the $dVGAT^{minos1}$ allele, and allow us to probe the adult mutant phenotype and the contributions of GABA release to adult visual behavior. We constructed a line containing the homozygous $dVGAT^{minos1}$ allele with *dVGAT-GAL4(II)*, *UAS-dVGAT(III)* and a temperature-sensitive version of the GAL4 transcriptional repressor GAL80 on chromosome III (McGuire et al., 2003) ($dVGAT^{minos1}$, *dVGAT-GAL4(II); UAS-dVGAT(III), tub-GAL80*^{ts}). The flies were cultured at 30°C, the permissive temperature for expression, until they had completed embryonic and larval development. They were then shifted to 18°C at 50% pupation to block further dVGAT expression. We refer to flies raised at 30°C then shifted to 18°C as dVGAT knockdowns. The knockdown flies (Fig. 6C, K.D.) showed *dVGAT* expression levels ~10–20% of flies that were maintained at 30°C and allowed to express dVGAT throughout development and adulthood (Fig. 6C, 30°C Rescue).

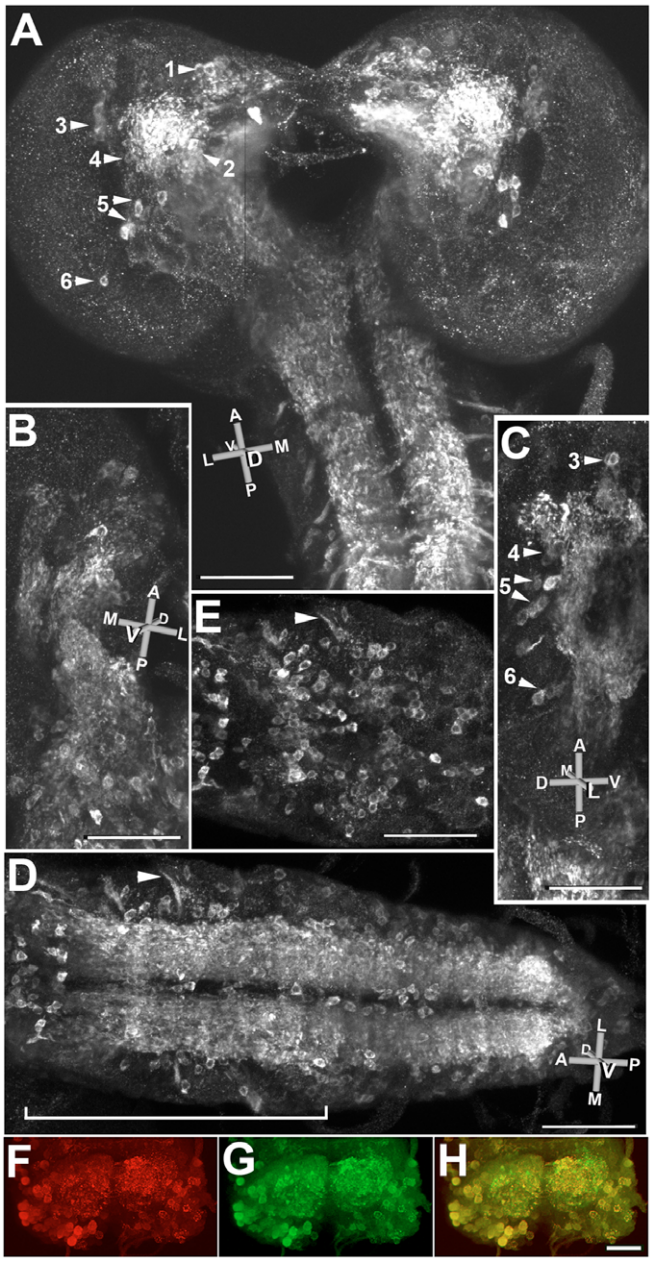

Fig. 4. Expression of dVGAT protein in larvae. (A) Confocal stacks from three combined, ×40 fields show a dorsal view of the brain and the anterior portion of the nerve cord. An orientation key is shown: L. lateral; M, medial; D, dorsal; V, ventral; A, anterior; P, posterior. (B) A ventral view of one half of the brain and the anterior portion of the nerve cord from a separate larva. (C) A side view (lateral to medial) of another larva showing the central brain. A small portion of the anterior nerve cord is visible at the bottom of the panel. Six clusters of GABAergic neurons are visible in the brain, labeled 1–6 in A, with clusters 3–6 visible in C. Note that cluster 2 in A is obscured by the intense labeling of the processes. (D) A ventral view of the nerve cord from another animal including optical sections through the entire depth of the nerve cord. A nerve root is indicated (arrowhead). (E) A subset of optical sections from the bracketed region in D reveals labeled cells on the ventral surface of the cord, with approx. 75 cells per abdominal segment. For comparison, in late stage embryos labeled with an antiserum to GABA, each segment was estimated to contain approx. 54 strongly and 50 weakly labeled neurons, ~20% of the total number of neurons per segment (Kuppers et al., 2003). (F–H) Co-labeling for dVGAT in red (F) and GABA in green (G) shows extensive co-localization (H, yellow) in both cell bodies and neuropil. As in D and E most cell bodies are near the ventrolateral surfaces of the cord. Scale bars, (A–E) 100 μm; (F–H) 50 μm.

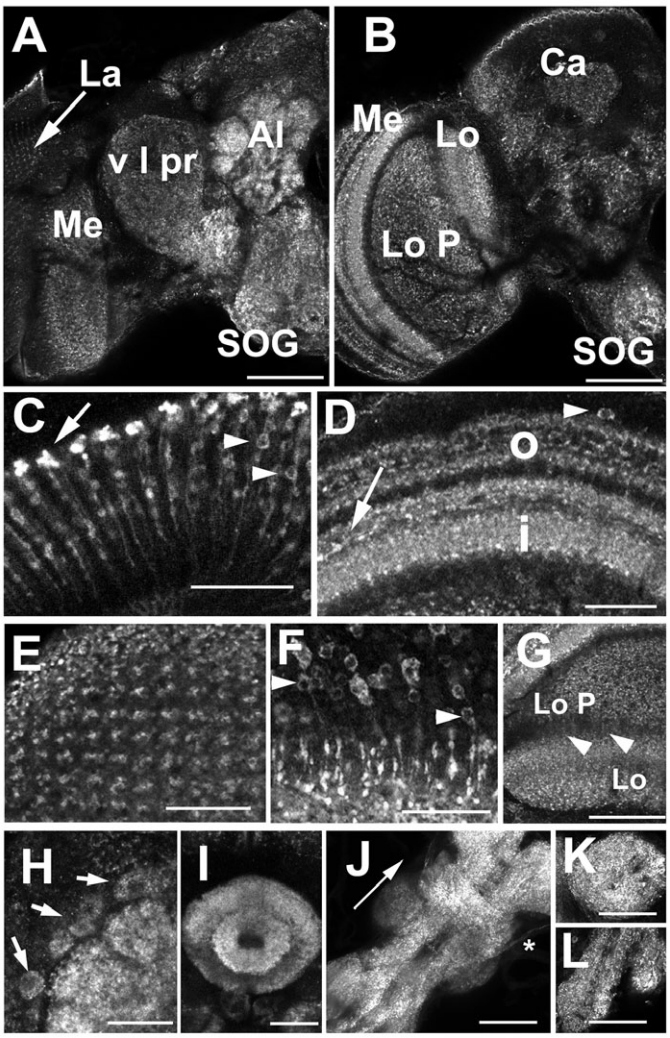

Fig. 5. Expression of dVGAT in the adult optic ganglia and brain. (A,B) Frontal views of an adult fly brain and optic lobes. An anterior optical section (A) shows punctate labeling in the glomeruli of the antennal lobe (Al), the subesophageal ganglion (SOG), ventral lateral protocerebrum (v l pr), and in the optic lobe, the lamina (La) and medulla (Me). A more posterior optical section (B) shows labeling of the lobula (Lo) and lobula plate (Lo P). Higher magnification images show morphologically distinct centrifugal projections of the C2 (C, arrow) and C3 cells (C, arrowheads) in the distal lamina. Labeling in the outer (D, o) and inner medulla (D, i) represent centrifugal processes from C2 and C3 cells, centripetal, putative transmedullary cells (D, arrowhead) (Sinakevitch and Strausfeld, 2004), as well as tangential GABAergic processes (Meyer et al., 1986; Sinakevitch and Strausfeld, 2004) (D, arrow). The retinotopic orientation of labeled processes in the outer medulla can be seen in a view toward the surface of the medulla (E), and is in part derived from the multiple, putative Tm cells (F) whose cell bodies are in the cortical rind of the medulla. (G) Thin processes (arrowheads) may traverse the space between the lobula plate (Lo P), labeled in a loose meshwork pattern, and the lobula (Lo) which appears more stratified than the lobula plate in this view. (H–L) Higher power images of the central brain show labeling of antennal lobe (H) and ellipsoid body (I). Labeled figures likely to be cell bodies are observed adjacent to the antennal lobe (H, arrows). (J) A stack of confocal images shows the dorsal aspect of the thoracic ganglion (arrow points anteriorly). Immunoreactive processes appear to be contained in at least one set of nerve roots (asterisk). Additional views show the prothoracic (K, ventral view) and abdominal (L, ventral view) segments of the ganglion. Scale bars, (A,B,G,J,K,L) 50 μm; (C,D,E,F,H,I) 20 μm.

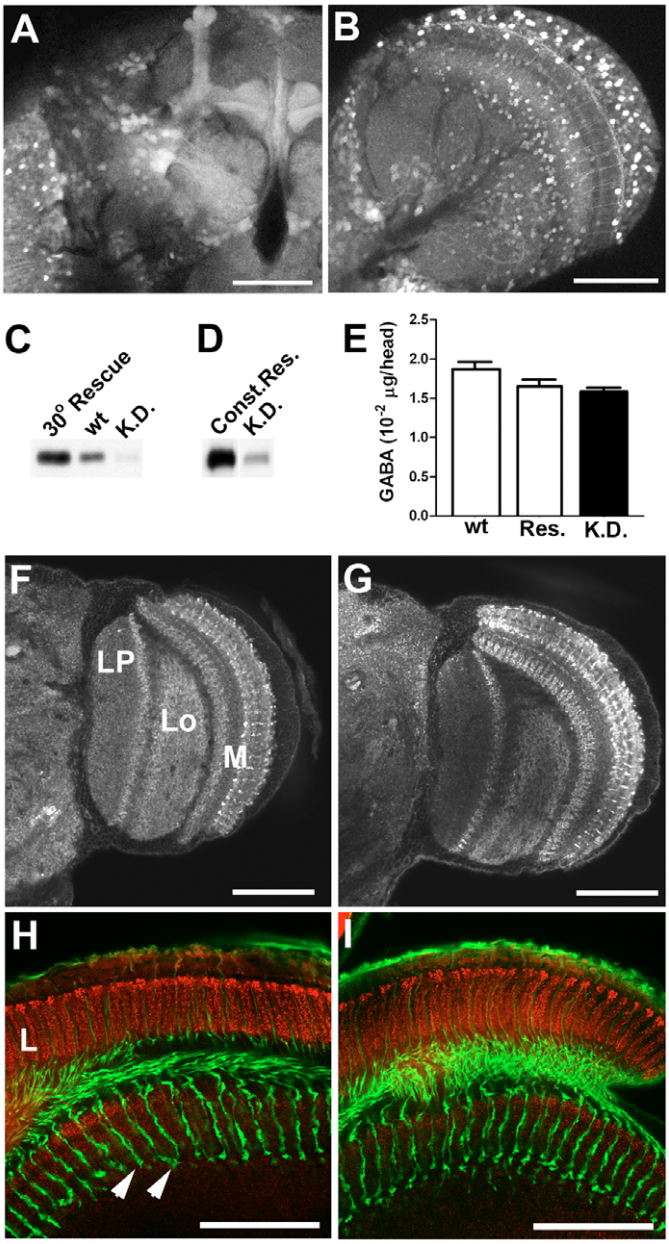

Fig. 6. Rescue using *dVGAT* transgenes. The expression pattern of *dVGAT-GAL4* drivers on chromosome II (A) or III (B) are shown using soluble GFP as a marker. (C) Western blots of *dVGAT*^{minos1}*, dVGAT-GAL4; UAS-dVGAT(III), tub-GAL80*^{ts} flies raised continuously at 30°C (30° Rescue) show high expression of dVGAT relative to flies shifted to 18°C at 50% pupation and then maintained at 18°C (K.D.; knockdown). Wild-type flies (wt; CS strain) raised at 25°C show an intermediate level of expression. (D) In a separate experiment *dVGAT*^{minos1}*, dVGAT-GAL4; UAS-dVGAT(III)* (constitutive rescue; *Const.Res.*) and *dVGAT*^{minos1}*, dVGAT-GAL4; UAS-dVGAT(III), tub-GAL80*^{ts} flies (K.D.) were shifted in parallel from 30° to 18°C at 50% pupation. The knockdown flies had lower levels of expression than the constitutively rescued flies. (E) HPLC analysis of heads from wild-type, knockdown and constitutively rescued controls (Res.) shows similar GABA contents. (F,G) Labeling for CSP in adult heads from constitutively rescued flies (F) cannot be distinguished from labeling in knockdown (G) flies. (H,I) Co-labeling using mAb nc82 (red) and anti-HRP (green) of adult heads from constitutively rescued controls (H) and knockdown (I) animals are indistinguishable. Labeled structures in F–I include the medulla (M), lobula (Lo), lobula plate (LP), lamina (L), and photoreceptor cell processes in the medulla (arrowheads). Scale bars, (A,B,F–I) 50 µm.

Constant exposure to 30°C limited the numbers of healthy flies (data not shown) available for further behavioral experiments. We therefore generated an additional control line in which *dVGAT* was constitutively rescued (*dVGAT*^{minos1}*, dVGAT-GAL4(II); UAS-dVGAT(III)*) regardless of temperature. Western blots showed that dVGAT expression in the knockdown line (Fig. 6D, K.D.) is ~10–20% that of the constitutively rescued flies (Fig. 6D, Const.Res.; differences in the relative intensity of the K.D. lane in Fig. 6C and D reflect differences in the exposure time for each blot).

To assess the potential impact of *dVGAT* knockdown on GABA storage we performed HPLC on heads of the constitutively rescued (Fig. 6E, Res.), knockdown (K.D.) and wild-type (wt) flies. We did not detect a significant difference in total GABA content between the three genotypes. However, it is unclear how this measure may compare with vesicular GABA content available for exocytotic release (see Discussion).

To determine whether knockdown of *dVGAT* would cause gross neuroanatomical changes, we immunolabeled adult brains from both knockdown and control (constitutively rescued) flies, focusing primarily on the optic lobes. The neuropil of the medulla, lobula and lobula plate in control (Fig. 6F) and knockdown (Fig. 6G) were labeled for CSP (Zinsmaier et al., 1990) and appear similar if not indistinguishable. The lamina and proximal medulla from control (Fig. 6H) and knockdown (Fig. 6I) animals are shown co-labeled with antibodies to the synaptic protein Bruchpilot (mAb nc82) (Wagh et al., 2006) and the neuronal marker Nervana (anti-HRP) (Sun and Salvatera, 1995), the latter highlighting the projections of the photoreceptor cell axons into the medulla. Although we cannot rule out subtle changes in connectivity or synaptic structure, the anatomy of the lamina and the organization of the photoreceptor cell processes appeared to be intact in the *dVGAT* knockdown flies.

General motion processing in *dVGAT* knockdown flies is intact

The survival of the *dVGAT* knockdown flies allowed us to test the effects of reduced dVGAT expression and GABA release on adult visual behavior. All experiments were performed 5–7 days after eclosion. As controls for most studies, including those shown in Fig. 7, we used the constitutively rescued flies. Controls were cultured in parallel and using the same temperature shift (30° to 18°C at 50% pupation) as for the knockdown line. We made use of a digital flight simulator to assess both general motor function and specific visual sub-systems. As a metric for the overall functional capacity of the flight motor system, we optically tracked wing motions and determined both total wing beat frequency and wing beat amplitude while animals were engaged in active visual flight control. Both knockdown and control (constitutively rescued) flies maintained normal (wild-type) ranges in frequency and amplitude (data not shown), suggesting that the neural regulation and resultant mechanical power output of the flight motor system was intact in the mutant flies (Gordon and Dickinson, 2006). These data indicate that reduced dVGAT expression does not result in systemic motor deficits – a critical prerequisite that enabled us to specifically examine visual flight behaviors. The lack of a gross effect on flight by the GABA-deficient *dVGAT* mutants is somewhat surprising, but consistent with the effects of abdominally injecting picrotoxin, which alters visuo-motor responses but not overt flight capacity in *Drosophila* (Bülthoff and Bülthoff, 1987) (see Discussion).

We used the flight simulator to perform several optomotor stabilization experiments. Flight control is simulated by coupling the fly's steering wing kinematics to the movement of the visual

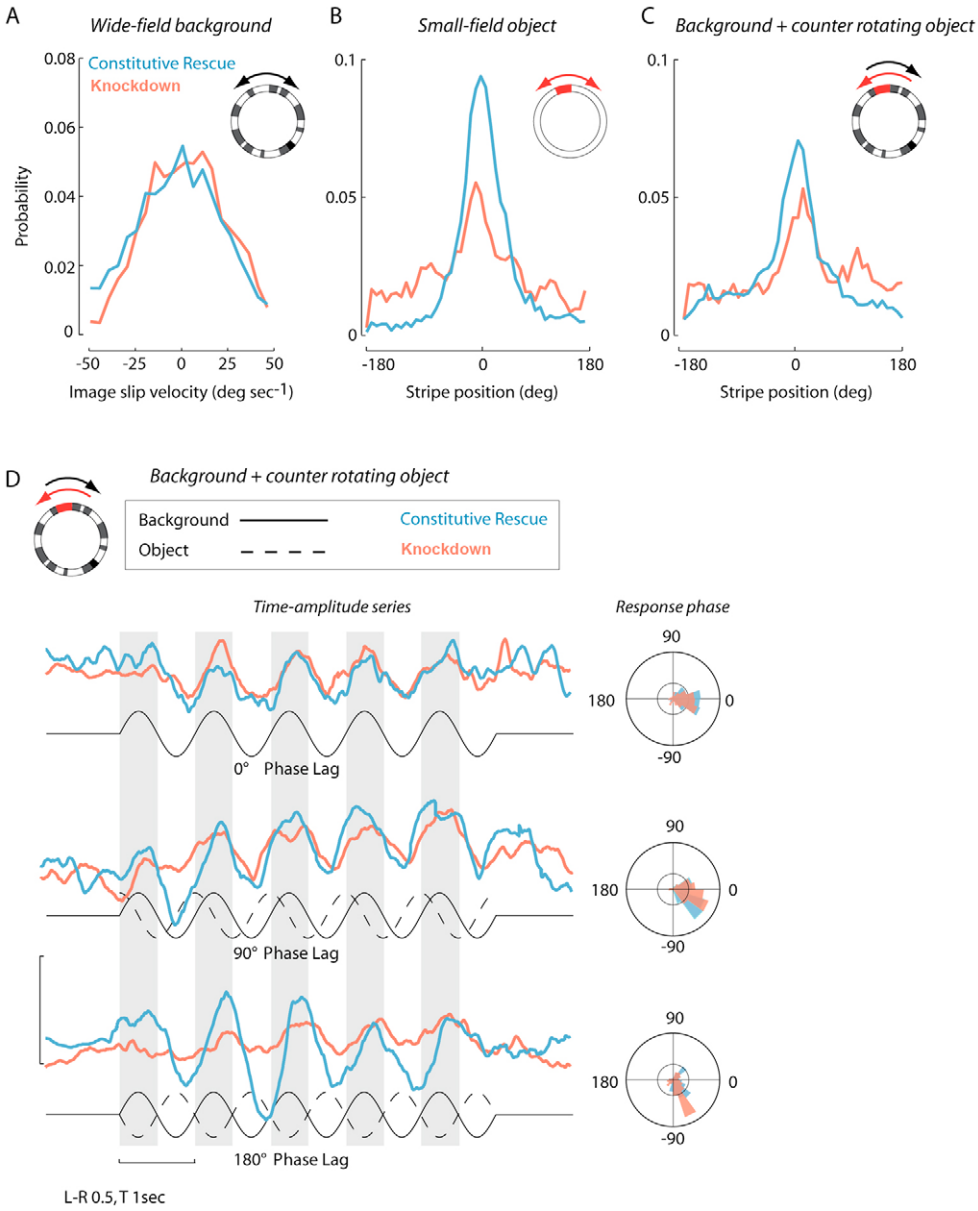

Fig. 7. Reduced dVGAT compromises visual object fixation behavior. All probability distributions are normalized to the number of data samples such that the cumulative probability equals 1. Statistical tests for (A–C): Kolmogorov–Smirnov two-sample test for probability distribution differences, *P*-values as indicated below. (A) Mean probability distributions of image slip velocity under conditions in which flies had closed-loop control biased with a sinusoid (see Materials and methods) over a wide-field high-contrast random checkerboard background panorama (inset cartoon). Knockdown (red) *N*=10; rescue (blue) *N*=15, *P*>0.3. (B) Under biased closed-loop conditions, the display was switched to a uniform white panorama with a single dark vertical stripe located by convention at the 0-degree position. Mean probability distributions of image position is indicated such that 0 deg. corresponds to the object being fixated directly in front of the fly. Knockdown *N*=15, rescue *N*=15, *P*<0.01. (C) Same as B, but now the small-field object (stripe) was coupled to the motion of the checkerboard background such that a clockwise movement of the object resulted in a counter-clockwise rotation of the background and *visa versa*. The two stimuli were 180 deg. out of phase. Knockdown *N*=15, rescue *N*=15, *P*<0.01. (D) Visual stimuli were delivered in open-loop conditions in which the fly had no control over the display, but reacted to the imposed sinusoidal motion by evoking wing steering kinematics, the difference in amplitude of the two wings (L–R; uncalibrated wing beat analyzer signal). As such, image velocity continually varied. We varied the phase lag between the vertical object (stripe) and the checkerboard background. Knockdown *N*=10, rescue *N*=15. The solid black line indicates background motion; the dashed line shows the object motion. Gray bars indicate periods of rightward (clockwise) motion. Upward deflections in L–R wing beat amplitude similarly indicate rightward turns. Unpaired Student's *t*-test, *P*>0.05 for 0 deg. and 90 deg. phase treatments, *P*<0.01 for 180 deg. treatment.

panorama. Under such conditions, wild-type flies robustly stabilize the visual panorama inbetween rapid turns, analogous to our own eye saccades. For our experiments, we added a sinusoidal bias to the feedback controller to ensure that the flies were actively engaged in controlling the visual display rather than passively flying forward (see Materials and Methods). Under these conditions for a wide-field (panoramic) display pattern, the mean image slip velocity is zero degrees per second. We compared the optomotor control capacity of knockdown and control flies in 20-second trials and found no significant differences between the slip velocity distributions (Fig. 7A). That is, the two groups were equally capable of stabilizing a wide-field panorama, which suggests that general

motion processing and optomotor control circuits are intact despite reduced dVGAT expression.

Visual figure detection is disrupted in *dVGAT* knockdown flies

In addition to general wide-field optomotor control, flies use both motion and position information to actively steer toward attractive features of the visual landscape, a 'perch approach' reflex that can be elicited in the flight simulator by an elongated vertical bar moving across the horizon (Maimon et al., 2008). Under dynamic closed-loop feedback conditions, a normal active fly steers to fixate the small-field stripe within the frontal portion of its retina. This reflex is robust enough that under conditions in which the animal is challenged with a sinusoidal bias added to the fly's active control, the resulting probability distribution of horizontal (azimuthal) stripe position is nevertheless tightly centered at zero degrees – directly forward in the visual field (Fig. 7B). Knockdown flies showed a reduced ability to fixate a stripe moving against a uniform white background as evidenced by a reduced peak and larger spread in the normalized distribution (Fig. 7B). Knockdown flies also showed a diminished capacity for tracking a stripe moving against a counter-rotating wide-field background in which any displacement of the stripe was matched exactly by motion of the background in the opposite direction (Fig. 7C). Thus, although the dVGAT-deficient flies show essentially wild-type wide-field optomotor reflexes, they exhibit difficulty in actively tracking a small object either in the presence or absence of concomitant background movement.

We further investigated the temporal response properties by varying the feedback dynamics of the object and the counter-rotating background under open-loop feedback conditions in which the fly had no control over the display (Fig. 7D). We generated three stimuli, one in which the object was phase-locked with the textured wide-field background (i.e. 0 deg. phase lag), generating a stimulus essentially identical to that used in Fig. 7A. The two additional stimuli used lags of 90 and 180 deg., the latter stimulus being identical to that used in Fig. 7C. In response to these stimuli, flies exhibited sinusoidal modulations in steering kinematics (left minus right wing beat amplitude, Fig. 7D) as they attempted to track the relative movement of the object. We find that the amplitude of behavioral responses by knockdown flies decreased progressively as the figure and ground were moved further out of phase (Fig. 7D), whereas the phase of behavioral responses were little impacted. The knockdown flies actively altered their wing kinematics to counteract sinusoidal bias in wide-field visual motion, just as they maintained zero-average slip velocity under fully closed-loop conditions (Fig. 7A). However, consistent with the closed-loop results, under biased conditions the same animals show reduced capacity to track the object when it moves with the background only 75% of the time (Fig. 7D 90 deg. lag), and severely degraded capacity when the object always moved in the opposite direction (Fig. 7D 180 deg. lag). Taken together, these results suggest that general wide-field optomotor function is intact, and the timing of visual signals is not significantly altered by *dVGAT* knockdown, whereas the behavioral deficit in the *dVGAT* knockdown flies is specific for figure detection computations required to follow or fixate the direction of gaze on a small-field object, and more so for the control of response magnitude rather than timing.

DISCUSSION

VGAT mutants provide an important model to investigate the contribution of GABA release to complex behavior. However, studies of VGAT mutants in other genetic systems have been limited. The *C. elegans* VGAT mutant *unc-47* primarily disrupts peripheral GABAergic circuits that innervate the neuromuscular junction (Schuske et al., 2004), and homozygous VGAT knockout mice die as embryos (Wojcik et al., 2006). To allow the study of VGAT in the fly, we have developed a new antibody to *Drosophila* VGAT, generated GAL4 and UAS transgenic lines to express dVGAT, characterized a *dVGAT* mutant and constructed a inducible rescue line in which the *dVGAT* transgene is expressed during development but not adulthood.

Previous pharmacological studies have suggested that GABA may regulate optomotor behavior in the fly (Bülthoff and Bülthoff, 1987; Egelhaaf et al., 1993; Warzecha et al., 1993), and we have used the *dVGAT* knockdown flies as a new genetic model to further test this hypothesis. Our behavioral results indicate that object detection is particularly sensitive to a decrease in GABA release and we discuss possible mechanisms below. *dVGAT* flies provide an important platform for dissecting the circuits underlying this phenotype, and more generally, allow further studies on the function of GABA release in a variety of other behaviors. We note that GAD, another marker commonly used to mark GABAergic cells is less specific than dVGAT, and is expressed in at least some glutamatergic cells (Featherstone et al., 2000).

The lethality of *dVGAT* larvae support the idea that dVGAT also plays an important role in development. In mice, the most prominent morphological phenotypes of both VGAT and GAD knockouts are non-neuronal, and include cleft palate (Condie et al., 1997; Ji et al., 1999; Wojcik et al., 2006). In the fly, RNAi-mediated knockdown of the GABA-B receptor alters tracheal morphology (Dzitoyeva et al., 2005), and *dVGAT* mutants also show a relatively splayed tracheal pattern (not shown) raising the possibility that GABA plays a non-neuronal role in embryonic development in the fly as well as mammals.

To circumvent the early developmental requirements for *dVGAT*, we used a temperature-sensitive repressor of GAL4 ($GAL80^{ts}$) to selectively knockdown expression in the adult. We constructed a line containing *dVGAT-GAL4, UAS-dVGAT* and a ubiquitously expressed $GAL80^{ts}$ transgene (*tub-*$GAL80^{ts}$) in the mutant *dVGAT* background to generate the inducible knockdown line $dVGAT^{minos1}$, *dVGAT-GAL4(II); UAS-dVGAT(III), tub-*$GAL80^{ts}$. The $GAL80^{ts}$ protein is functional at 18°C, thereby blocking the transcriptional activation of the *UAS-dVGAT* transgene by GAL4. Conversely, at 30°C, $GAL80^{ts}$ is non-functional and the *UAS-dVGAT* transgene is activated. Thus, we generated an inducible knockdown line in which the embryonic lethality of *dVGAT* mutant could be rescued, but *dVGAT* expression could be knocked down at later stages by shifting the flies from 30° to 18° C.

Shifting the flies from 30° to 18°C during embryonic or larval stages did not yield any viable adults (data not shown) suggesting that *dVGAT* is required throughout larval development. We were surprised to find that shifting adult flies to 18°C for up to 1 week did not reduce dVGAT expression (data not shown). Other workers have been able to use $GAL80^{ts}$ to effectively reduce protein expression using as little as 1 h of exposure to the restrictive temperature (McGuire et al., 2003). It would appear that the dVGAT protein persisted despite the blockade of expression from the transgene. In other words, dVGAT showed a dramatic degree of perdurance.

We hypothesized that the apparent perdurance of dVGAT might be due to limited recycling of the protein in the adult. To circumvent this problem, and still allow expression during development, we took advantage of the restructuring of the nervous system during metamorphosis. During pupal stages, some of the larval nervous system is destroyed, and those aspects of the CNS used only in the

adult develop from immature precursor cells. We speculate that by shifting to the restrictive temperature during pupation, we blocked *de novo* adult dVGAT expression before it could occur, thus circumventing problems with perdurance. We note that other vesicular transporters such as *dVMAT* appear to be similarly resistant to knockdown as adults (A.C. and D.E.K., manuscript in preparation). Vesicular transporters are transmembrane proteins, and must be processed in the ER and Golgi in the cell body before trafficking to synaptic vesicles at the nerve terminal. Importantly, SVs undergo multiple rounds of recycling at the nerve terminal, and the processes by which SV proteins might be degraded or leave the nerve terminal are not known. Future experiments using vesicular transporter mutants defective in membrane trafficking may help address this question, and perhaps help to explain the perdurance of dVGAT.

Using HPLC, we did not detect a decrease in the total tissue content of GABA in heads of adult *dVGAT* knockdown flies. To our knowledge, GABA content has not been measured in either VGAT knockout mice or *C. elegans* mutants, but flies containing a *dVMAT* loss-of-function mutation, as well as VMAT2 knockout mice show dramatically reduced monoamine contents (Simon et al., 2008; Fon et al., 1997). These data suggest that in some cases, neurotransmitter that is not packaged into vesicles is degraded. However, the *C. elegans* VAChT mutant *unc-17* shows an increase rather than a decrease in total tissue acetylcholine content (Hosono et al., 1987). Thus, unlike the monoamines, acetylcholine that is not packaged into synaptic vesicles may not be degraded. We have measured GABA content in a *dVGAT* knockdown fly rather than a true null mutant, and it is possible that our inability to detect a change in GABA content reflects the presence of residual VGAT activity. Alternatively, our results may suggest that GABA behaves differently than either acetylcholine or monoamine neurotransmitters. Further work will be needed to determine the fate of GABA in the absence of VGAT, and the relationship between total tissue GABA and the vesicular GABA content available for exocytotic release.

dVGAT is expressed widely in the adult insect nervous system, and the functions of several GABAergic circuits in the central brain have been previously investigated. Cell bodies adjacent to the antennal lobe that express dVGAT are likely to represent local GABAergic interneurons, also present in other insects (Distler and Boeckh, 1997). These cells are thought to regulate cross-talk between adjacent glomeruli and hone the fly's olfactory response to specific odors (Olsen and Wilson, 2008; Silbering and Galizia, 2007; Wilson and Laurent, 2005). dVGAT is also expressed in the central complex, consistent with reports using other GABAergic markers (Harrison et al., 1996; Homberg et al., 1987; Meyer et al., 1986) and may contribute to the role of GABA release in spatial working memory (Neuser et al., 2008). We also observed labeling for dVGAT in the calyx of the mushroom bodies, where GABAergic input may regulate Kenyon cell activity and olfactory learning (Homberg et al., 1987; Leitch and Laurent, 1996; Liu et al., 2007; Strambi et al., 1998; Yasuyama et al., 2002). We anticipate that *dVGAT* knockdown flies may be used to further explore the contribution of GABA release to these behaviors. Here we focus primarily on dVGAT expression in the optic ganglia and its possible contribution to motion detection.

Some 1500 neurons in each optic lobe have been suggested to store GABA (Buchner et al., 1988) and a subset of these have been morphologically characterized in *Drosophila* and/or larger flies. The somata of C2- and C3-type cells are distal to the lamina and project centrifugally toward the retina. Both types label for GABA and/or GAD (Buchner et al., 1988; Datum et al., 1986; Enell et al., 2007; Kolodziejczyk et al., 2008; Sinakevitch et al., 2003) and both arborize in the medulla as well as the lamina (Morante and Desplan, 2008). The terminal of each C2 cell forms a rosette-like structure in the distal aspect of the lamina whereas C3 cells have multiple, more proximal boutons (Fischbach and Dittrich, 1989). Since anti-dVGAT labels the terminals of both C2 and C3 cells, it is likely that GABA is released presynaptically at both of these sites and may regulate the function of laminar monopolar neurons innervated by these cells (Takemura et al., 2008). The laminar monopolar neurons have been implicated in motion detection (Rister et al., 2007), raising the possibility that C2 and C3 may also contribute in some way to this process.

Large numbers of somata distal to the medulla (~900/optic lobe) label for GABA and GAD (Buchner et al., 1988; Sinakevitch and Strausfeld, 2004) and as shown here, for dVGAT, but their identity remains unclear. At least 35 morphologically defined cell types reside within the cortical rind of the medulla (Fischbach and Dittrich, 1989; Takemura et al., 2008). Cells immunoreactive for GABA (Sinakevitch and Strausfeld, 2004) and dVGAT may be transmedullary (Tm) cells that extend through the medulla and into the lobula plate, and could be identical to Tm9 (Sinakevitch and Strausfeld, 2004). However, it is difficult to trace their projections and to determine whether they are indeed transmedullary and project into the lobula or rather terminate within the neuropil of the medulla. Molecular genetic methods have been used to elegantly tease out the circuitry encoding color vision in the medulla (Gao et al., 2008; Morante and Desplan, 2008), and we anticipate that similar methods will help determine the projections of the putative Tm cells that express dVGAT.

In addition to possible retinotopic projections, dVGAT labelings in the lobula and lobula plate are likely to include tangentially projecting cells previously shown to label for GABA and/or GAD (Meyer et al., 1986; Sinakevitch and Strausfeld, 2004). It has been proposed that tangentially projecting cells in either the lobula (Sinakevitch and Strausfeld, 2004) and/or lobula plate are critical for motion detection (Brotz and Borst, 1996; Brotz et al., 2001). However, the circuitry responsible for motion detection and the sites at which GABA may contribute to this process are not clear.

As originally proposed some 50 years ago, motion detection may be modeled using a series of retinotopic elementary motion detectors (EMDs), each of which encodes luminance fluctuations detected by neighboring retinotopic columns in the optic ganglia (Hassenstein and Reichardt, 1956; Reichardt, 1987; Rister et al., 2007). Inhibitory signals presumably mediated by GABA are thought to be essential for modeling interactions between mirror image subunits of the EMDs (Hassenstein and Reichardt, 1956; Reichardt, 1987; Rister et al., 2007). However, the cellular nature of the EMD is not fully understood. Whereas monopolar cells segregate visual information and contribute to early motion pre-processing (Coombe and Heisenberg, 1986; Rister et al., 2007; Zhu et al., 2009), it remains controversial as to whether motion computations are solely made within the deeper visual ganglia, the lobula (Sinakevitch and Strausfeld, 2004), and/or lobula plate (Brotz and Borst, 1996; Brotz et al., 2001).

In the lobula plate, both horizontal and vertical tangential cells (HS and VS) express the GABA-A RDL receptor, and both are adjacent to GABAergic terminals in *Drosophila* and larger flies (Brotz and Borst, 1996; Raghu et al., 2007). Despite intense study, a retinotopic source for inhibitory signals to the LPTCs) – possibly contributing to elementary motion detection – remains elusive. By contrast, it is clear that GABA is released from intrinsic centrifugal horizontal (CH) cells in the lobula plate (Eckert and Dvorak, 1983), and that CH cells play an important role in some aspects of motion

detection (Eckert and Dvorak, 1983; Egelhaaf, 1985; Gauck et al., 1997; Hausen, 1984). Both cell ablation and pharmacologic studies using picrotoxin indicate that GABA release from CH cells is required for the small field tuning of the figure detection cell FD1 (Egelhaaf et al., 1993; Warzecha et al., 1993). Application of picrotoxin also disrupts the function of HS, VS and other LPTCs (Egelhaaf et al., 1990; Gilbert, 1990; Kondoh et al., 1995; Schmid and Bülthoff, 1988). More generally, injection of picrotoxin into the abdomen of *Drosophila* inverts the polarity of both the cellular and behavioral response to movement (Bülthoff and Bülthoff, 1987). These studies support the idea that GABA is critical to motion detection and visual behavior in flies, but aside from CH cells, the functions of other GABAergic cells are not known.

We find that knockdown of *dVGAT* causes a relatively specific deficit in figure detection without significantly compromising flight or more wide-field optomotor behavior. Adult *Drosophila* injected with the GABA receptor antagonist picrotoxin also show a relatively specific deficit in figure detection (Bülthoff and Bülthoff, 1987). The similarity between the *dVGAT* knockdown phenotype and the behavior of adult flies injected with picrotoxin suggests that the defect we observe in the *dVGAT* knockdown flies is the result of decreased GABAergic signaling in the adult. However, it is also possible that *dVGAT* knockdown during pupation, or perhaps in the newly eclosed adult (Barth et al., 1997) causes a developmental defect that contributes to the adult visual phenotype. Although we find the nervous system of the knockdown flies is grossly intact, we cannot rule out subtle differences in connectivity or synaptic function. Ideally, to circumvent this problem, we would perform additional experiments in which *dVGAT* was knocked down in the adult fly without reducing expression during development. Unfortunately, the apparent perdurance of dVGAT protein (see above) has prevented us from performing these experiments. In future studies, it may be possible to use other molecular genetic techniques to selectively knockdown *dVGAT* in the adult and to tease out the potential developmental effects of *dVGAT* on adult behavior.

Whether or not the knockdown of *dVGAT* effects development, or only restricts GABA release in the adult fly, the relative specificity of the adult phenotype is surprising. The neuropil of both the thoracic and optic ganglia as well as the central brain are densely packed with processes expressing dVGAT and other markers for GABAergic neurotransmission, and it is unlikely that GABA release is only involved in a single behavior. Why should figure detection be more sensitive than other behaviors to a reduction in GABAergic signaling? It is possible that the GAL4 drivers we used here express dVGAT only in a selected subset of cells that rescue viability and wide field motion, but not those required for object detection. In this case, our results would suggest that we have uncovered a novel circuit devoted to object detection. Alternatively, the circuits required for computation of object motion may somehow be more sensitive to changes in GABAergic signaling. Further genetic mapping studies using the *dVGAT* mutants and transgenes will help to clarify these issues and to identify the inhibitory circuits enabling motion computation in the fly. These studies will be facilitated by the ability to spatially restrict dVGAT expression using variants of the GAL/UAS system, and RNAi lines for *dVGAT* that have recently become available from The Vienna *Drosophila* RNAi Center (http://www.vdrc.at/).

Which GABAergic circuits (in the mature adult or during development) might be disrupted in the *dVGAT* knockdown flies? CH cells in the lobula plate have been shown to be involved in detection of moving objects against a moving background (Egelhaaf and Borst, 1993; Warzecha et al., 1993). It is therefore conceivable that the detection of all object movement is mediated by interactions between CH and FD cells. Conversely, it is possible that some of the other ~1500 GABAergic cells in the optic ganglia contribute to the *dVGAT* phenotype. C2 neurons may be involved in orientation (Douglass and Strausfeld, 1995) and both C2 and C3 provide input to monopolar neurons (Takemura et al., 2008), which have been suggested to function as motion detectors (Rister et al., 2007). *dVGAT* mutants and transgenes will facilitate further tests to determine how GABA release from C2, and other cells in the optic ganglia may contribute to motion detection.

A number of recent reports have demonstrated the value of *Drosophila* genetics in investigating the behavioral importance of GABAergic signaling in the central nervous system (Agosto et al., 2008; Dzitoyeva et al., 2003; Hamasaka et al., 2005; Liu et al., 2007; Su and O'Dowd, 2003; Wilson and Laurent, 2005). Our results complement these studies and allow us to assess, for the first time, the effects of decreasing the function of dVGAT and presynaptic GABA release on fly behavior. We anticipate that further studies of *dVGAT* will be useful to investigate the effects of GABA release on a variety of behaviors in the fly, including olfaction (Olsen and Wilson, 2008; Silbering and Galizia, 2007; Wilson and Laurent, 2005), learning (Liu et al., 2007) and sleep (Agosto et al., 2008).

LIST OF SYMBOLS AND ABBREVIATIONS

BDGP	Berkeley *Drosophila* Genome Project
CH	centrifugal horizontal
CSP	Cysteine string protein (CSP)
EMD	elementary motion detector
FD	figure detection
GABA	gamma amino butyric acid
GAD	glutamic acid decarboxylase
GHB	gamma hydroxy butyrate
HS	horizontal system
LPTC	lobula plate tangential cell
Tm	transmedullary
VGAT	vesicular GABA transporter
VIAAT	vesicular inhibitory amino acid transporter
VS	vertical system

ACKNOWLEDGEMENTS

The authors acknowledge the helpful discussions from members of the Krantz, Frye and Simpson labs and the expert technical assistance of George Lawless in the Krantz lab. The work was supported by grants from the EJLB Foundation, the National Institute of Mental Health (D.E.K.), HHMI and the National Science Foundation IOS-0718325 (M.A.F.), a Helen Hay Whitney Post-Doctoral Fellowship, funding from L'Oreal Women in Science, the Howard Hughes Medical Institute (J.H.S.) and The Edith Hyde Fellowship (D.M.C.). M.A.F. is a HHMI Early Career Scientist. Deposited in PMC for release after 6 months.

REFERENCES

Agosto, J., Choi, J. C., Parisky, K. M., Stilwell, G., Rosbash, M. and Griffith, L. C. (2008). Modulation of GABA(A) receptor desensitization uncouples sleep onset and maintenance in Drosophila. *Nat. Neurosci.* **11**, 354-359.

Barth, M., Hirsch, H. V., Meinertzhagen, I. A. and Heisenberg, M. (1997). Experience-dependent developmental plasticity in the optic lobe of *Drosophila melanogaster*. *J. Neurosci.* **17**, 1493-1504.

Borst, A. and Haag, J. (2002). Neural networks in the cockpit of the fly. *J. Comp. Physiol. A Neuroethol. Sens. Neural. Behav. Physiol.* **188**, 419-437.

Boschek, C. B. (1971). On the fine structure of the peripheral retina and lamina ganglionaris of the fly, *Musca domestica*. *Z. Zellforsch. Mikrosk. Anat.* **118**, 369-409.

Brand, A. H. and Perrimon, N. (1993). Targeted gene expression as a means of altering cell fates and generating dominant phenotypes. *Development* **118**, 401-415.

Brenner, S. (1974). The genetics of *Caenorhabditis elegans*. *Genetics* **77**, 71-94.

Brotz, T. M. and Borst, A. (1996). Cholinergic and GABAergic receptors on fly tangential cells and their role in visual motion detection. *J. Neurophysiol.* **76**, 1786-1799.

Brotz, T. M., Gundelfinger, E. D. and Borst, A. (2001). Cholinergic and GABAergic pathways in fly motion vision. *BMC Neurosci.* **2**, 1.

Buchner, E., Bader, R., Buchner, S., Cox, J., Emson, P. C., Flory, E., Heizmann, C. W., Hemm, S., Hofbauer, A. and Oertel, W. H. (1988). Cell-specific immuno-probes for the brain of normal and mutant *Drosophila melanogaster*. I. Wildtype visual system. *Cell Tissue Res.* **253**, 357-370.

Bülthoff, H. and Bülthoff, I. (1987). GABA-antagonist inverts movement and object detection in flies. *Brain Res.* **407**, 152-158.
Chang, H.-Y., Grygoruk, A., Brooks, E. S., Ackerson, L. C., Maidment, N. T., Bainton, R. J. and Krantz, D. E. (2006). Over-expression of the Drosophila vesicular monoamine transporter increases motor activity and courtship but decreases the behavioral response to cocaine. *Molecular Psychiatry* **11**, 99-113.
Clift-O'Grady, L., Linstedt, A. D., Lowe, A. W., Grote, E. and Kelly, R. B. (1990). Biogenesis of synaptic vesicle-like structures in a pheochromocytoma cell line PC12. *J. Cell Biol.* **110**, 1693-1703.
Condie, B. G., Bain, G., Gottlieb, D. I. and Capecchi, M. R. (1997). Cleft palate in mice with a targeted mutation in the gamma-aminobutyric acid-producing enzyme glutamic acid decarboxylase 67. *Proc. Natl. Acad. Sci. USA* **94**, 11451-11455.
Coombe, P. E. and Heisenberg, M. (1986). The structural brain mutant Vacuolar medulla of *Drosophila melanogaster* with specific behavioral defects and cell degeneration in the adult. *J. Neurogenet.* **3**, 135-158.
Daniels, R. W., Collins, C. A., Gelfand, M. V., Dant, J., Brooks, E. S., Krantz, D. E. and DiAntonio, A. (2004). Increased expression of the Drosophila vesicular glutamate transporter leads to excess glutamate release and a compensatory decrease in quantal content. *J. Neurosci.* **24**, 10466-10474.
Datum, K.-H., Weiler, R. and Zettler, F. (1986). Immunocytochemical demonstration of gamma-aminobutyric acid and glutamic acid decarboxylase in R7 photoreceptors and C2 centrifugal fiberes in the blowfly visual system. *J. Comp. Physiol.* **159**, 241-249.
Distler, P. G. and Boeckh, J. (1997). Synaptic connections between identified neuron types in the antennal lobe glomeruli of the cockroach, *Periplaneta americana*: II. Local multiglomerular interneurons. *J. Comp. Neurol.* **383**, 529-540.
Douglass, J. K. and Strausfeld, N. J. (1995). Visual motion detection circuits in flies: peripheral motion computation by identified small-field retinotopic neurons. *J. Neurosci.* **15**, 5596-5611.
Duistermars, B. J., Reiser, M. B., Zhu, Y. and Frye, M. A. (2007). Dynamic properties of large-field and small-field optomotor flight responses in Drosophila. *J. Comp. Physiol. A Neuroethol. Sens. Neural. Behav. Physiol.* **193**, 787-799.
Dzitoyeva, S., Dimitrijevic, N. and Manev, H. (2003). Gamma-aminobutyric acid B receptor 1 mediates behavior-impairing actions of alcohol in Drosophila: adult RNA interference and pharmacological evidence. *Proc. Natl. Acad. Sci. USA* **100**, 5485-5490.
Dzitoyeva, S., Gutnov, A., Imbesi, M., Dimitrijevic, N. and Manev, H. (2005). Developmental role of GABAB(1) receptors in Drosophila. *Brain. Res. Dev. Brain. Res.* **158**, 111-114.
Eckert, H. and Dvorak, D. R. (1983). The centrifugal horizontal cells in the lobula plate of the blowfly. *J. Insect Physiol.* **29**, 547-560.
Egelhaaf, M. (1985). On the neuronal basis of figure-ground discrimination by relative motion in the visual system of the fly II. Figure-detection cells, a new class of interneurons. *Biol. Cybern.* **52**, 195-209.
Egelhaaf, M. and Borst, A. (1993). A look into the cockpit of the fly: visual orientation, algorithms, and identified neurons. *J. Neurosci.* **13**, 4563-4574.
Egelhaaf, M., Borst, A. and Pilz, B. (1990). The role of GABA in detecting visual motion. *Brain Res.* **509**, 156-160.
Egelhaaf, M., Borst, A., Warzecha, A. K., Flecks, S. and Wildemann, A. (1993). Neural circuit tuning fly visual neurons to motion of small objects. II. Input organization of inhibitory circuit elements revealed by electrophysiological and optical recording techniques. *J. Neurophysiol.* **69**, 340-351.
Enell, L., Hamasaka, Y., Kolodziejczyk, A. and Nässel, D. R. (2007). gamma-Aminobutyric acid (GABA) signaling components in Drosophila: immunocytochemical localization of GABA(B) receptors in relation to the GABA(A) receptor subunit RDL and a vesicular GABA transporter. *J. Comp. Neurol.* **505**, 18-31.
Featherstone, D. E., Rushton, E. M., Hilderbrand-Chae, M., Phillips, A. M., Jackson, F. R. and Broadie, K. (2000). Presynaptic glutamic acid decarboxylase is required for induction of the postsynaptic receptor field at a glutamatergic synapse. *Neuron* **27**, 71-84.
Fischbach, K. F. and Dittrich, A. P. M. (1989). The optic lobe of Drosophila melanogaster. I. A Golgi analysis of wild type structure. *Cell Tissue Res.* **258**, 441-475.
Fon, E. A., Pothos, E. N., Sun, B. C., Killeen, N., Sulzer, D. and Edwards, R. H. (1997). Vesicular transport regulates monoamine storage and release but is not essential for amphetamine action. *Neuron* **19**, 1271-1283.
Gao, S., Takemura, S. Y., Ting, C. Y., Huang, S. Y., Lu, Z., Luan, H., Rister, J., Thum, A. S., Yang, M., Hong, S. T., et al., (2008). Neural substrate of spectral preference in Drosophila. *Neuron* **60**, 328-342.
Gasnier, B. (2004). The SLC32 transporter, a key protein for the synaptic release of inhibitory amino acids. *Pflugers Arch.* **447**, 756-759.
Gauck, V., Egelhaaf, M. and Borst, A. (1997). Synapse distribution on VCH, an inhibitory, motion-sensitive interneuron in the fly visual system. *J. Comp. Neurol.* **381**, 489-499.
Gilbert, C. (1990). Membrane conductance changes associated with the response of motion sensitive insect visual neurons. *Z. Naturforsch. [C]* **45**, 1222-1224.
Gordon, S. and Dickinson, M. H. (2006). Role of calcium in the regulation of mechanical power in insect flight. *Proc. Natl. Acad. Sci. USA* **103**, 4311-4315.
Greer, C. L., Grygoruk, A., Patton, D. E., Ley, B., Romero-Calderón, R., Chang, H.-Y., Houshyar, R., Bainton, R. J., DiAntonio, A. and Krantz, D. E. (2005). A splice variant of the Drosophila vesicular monoamine transporter contains a conserved trafficking domain and functions in the storage of dopamine, serotonin and octopamine. *J. Neurobiol.* **64**, 239-258.
Hamasaka, Y., Wegener, C. and Nässel, D. R. (2005). GABA modulates Drosophila circadian clock neurons *via* GABAB receptors and decreases in calcium. *J. Neurobiol.* **65**, 225-240.
Harrison, J. B., Chen, H. H., Sattelle, E., Barker, P. J., Huskisson, N. S., Rauh, J. J., Bai, D. and Sattelle, D. B. (1996). Immunocytochemical mapping of a C-terminus anti-peptide antibody to the GABA receptor subunit, RDL in the nervous system in *Drosophila melanogaster*. *Cell Tissue Res.* **284**, 269-278.
Hassenstein, B. and Reichardt, W. (1956). Systemtheoretische Analyses der Zeit-Reihenfolgen- und Vorzeichenauswertung bei der Bewegungsperzeption des Rüsselkäfers Chlorophanus. *Z. Naturforsch.* **11**, 513-524.
Hausen, K. (1984). The lobula-complex of the fly: structure, function and significance in visual behavior. In *Photoreception and Vision in Invertebrates* (ed. M. A. Ali), pp. 523-559. New York: Plenum.
Heisenberg, M. and Wolf, R. (1984). *Vision in Drosophila: Genetics of Microbehavior.* Berlin: Springer-Verlag.
Homberg, U., Kingan, T. G. and Hildebrand, J. G. (1987). Immunocytochemistry of GABA in the brain and suboesophageal ganglion of *Manduca sexta*. *Cell Tissue Res.* **248**, 1-24.
Hosono, R., Sassa, T. and Kuno, S. (1987). Mutations affecting acetylcholine levels in the nematode *Caenorhabditis elegans*. *J. Neurochem.* **49**, 1820-1823.
Ji, F., Kanbara, N. and Obata, K. (1999). GABA and histogenesis in fetal and neonatal mouse brain lacking both the isoforms of glutamic acid decarboxylase. *Neurosci. Res.* **33**, 187-194.
Kanner, B. I. (2006). Structure and function of sodium-coupled GABA and glutamate transporters. *J. Membr. Biol.* **213**, 89-100.
Kolodziejczyk, A., Sun, X., Meinertzhagen, I. A. and Nässel, D. R. (2008). Glutamate, GABA and acetylcholine signaling components in the lamina of the Drosophila visual system. *PLoS ONE* **3**, e2110.
Kondoh, Y., Hasegawa, Y., Okuma, J. and Takahashi, F. (1995). Neural computation of motion in the fly visual system: quadratic nonlinearity of responses induced by picrotoxin in the HS and CH cells. *J. Neurophysiol.* **74**, 2665-2684.
Kuppers, B., Sanchez-Soriano, N., Letzkus, J., Technau, G. M. and Prokop, A. (2003). In developing Drosophila neurones the production of gamma-amino butyric acid is tightly regulated downstream of glutamate decarboxylase translation and can be influenced by calcium. *J. Neurochem.* **84**, 939-951.
Leitch, B. and Laurent, G. (1996). GABAergic synapses in the antennal lobe and mushroom body of the locust olfactory system. *J. Comp. Neurol.* **372**, 487-514.
Liu, X., Krause, W. C. and Davis, R. L. (2007). GABAA receptor RDL inhibits Drosophila olfactory associative learning. *Neuron* **56**, 1090-1102.
Maimon, G., Straw, A. D. and Dickinson, M. H. (2008). A simple vision-based algorithm for decision making in flying Drosophila. *Curr. Biol.* **18**, 464-470.
McGuire, S. E., Le, P. T., Osborn, A. J., Matsumoto, K. and Davis, R. L. (2003). Spatiotemporal rescue of memory dysfunction in Drosophila. *Science* **302**, 1765-1768.
McIntire, S. L., Reimer, R. J., Schuske, K., Edwards, R. H. and Jorgensen, E. M. (1997). Identification and characterization of the vesicular GABA transporter. *Nature* **389**, 870-876.
Meinertzhagen, I. A. and O'Neil, S. D. (1991). Synaptic organization of columnar elements in the lamina of the wild type in *Drosophila melanogaster*. *J. Comp. Neurol.* **305**, 232-263.
Metaxakis, A., Oehler, S., Klinakis, A. and Savakis, C. (2005). Minos as a genetic and genomic tool in *Drosophila melanogaster*. *Genetics* **171**, 571-581.
Meyer, E. P., Matute, C., Streit, P. and Nässel, D. R. (1986). Insect optic lobe neurons identifiable with monoclonal antibodies to GABA. *Histochemistry* **84**, 207-216.
Morante, J. and Desplan, C. (2008). The color-vision circuit in the medulla of Drosophila. *Curr. Biol.* **18**, 553-565.
Muller, C., Viry, S., Miehe, M., Andriamampandry, C., Aunis, D. and Maitre, M. (2002). Evidence for a gamma-hydroxybutyrate (GHB) uptake by rat brain synaptic vesicles. *J. Neurochem.* **80**, 899-904.
Murphy, N. P. and Maidment, N. T. (1999). Orphanin FQ/nociceptin modulation of mesolimbic dopamine transmission determined by microdialysis. *J. Neurochem.* **73**, 179-186.
Neuser, K., Triphan, T., Mronz, M., Poeck, B. and Strauss, R. (2008). Analysis of a spatial orientation memory in Drosophila. *Nature* **453**, 1244-1247.
Olsen, S. R. and Wilson, R. I. (2008). Lateral presynaptic inhibition mediates gain control in an olfactory circuit. *Nature* **452**, 956-960.
Raghu, S. V., Joesch, M., Borst, A. and Reiff, D. F. (2007). Synaptic organization of lobula plate tangential cells in Drosophila: gamma-aminobutyric acid receptors and chemical release sites. *J. Comp. Neurol.* **502**, 598-610.
Reichardt, W. (1987). Evaluation of optical motion information by movement detectors. *J. Comp. Physiol. A* **161**, 533-547.
Rister, J., Pauls, D., Schnell, B., Ting, C. Y., Lee, C. H., Sinakevitch, I., Morante, J., Strausfeld, N. J., Ito, K. and Heisenberg, M. (2007). Dissection of the peripheral motion channel in the visual system of *Drosophila melanogaster*. *Neuron* **56**, 155-170.
Romero-Calderón, R., Shome, R. M., Simon, A. F., Daniels, R. W., DiAntonio, A. and Krantz, D. E. (2007). A screen for neurotransmitter transporters expressed In the visual system of *Drosophila melanogaster* identifies three novel genes. *Dev. Neurobiol.* **67**, 550-569.
Sagne, C., El Mestikawy, S., Isambert, M. F., Hamon, M., Henry, J. P., Giros, B. and Gasnier, B. (1997). Cloning of a functional vesicular GABA and glycine transporter by screening of genome databases. *FEBS Lett.* **417**, 177-183.
Schäfer, S. and Bicker, G. (1986). Common projection areas of 5-HT- and GABA-like immunoreactive fibers in the visual system of the honeybee. *Brain Res.* **380**, 368-370.
Schmid, A. and Bülthoff, H. (1988). Using neuropharmacology to distinguish between excitatory and inhibitory movement detection mechanisms in the fly *Calliphora eryhthrocephala*. *Biol. Cybern.* **59**, 71-80.
Schousboe, A. (2000). Pharmacological and functional characterization of astrocytic GABA transport: a short review. *Neurochem. Res.* **25**, 1241-1244.
Schuske, K., Beg, A. A. and Jorgensen, E. M. (2004). The GABA nervous system in *C. elegans*. *Trends Neurosci.* **27**, 407-414.
Sharma, Y., Cheung, U., Larsen, E. W. and Eberl, D. F. (2002). PPTGAL, a convenient Gal4 P-element vector for testing expression of enhancer fragments in drosophila. *Genesis* **34**, 115-118.
Silbering, A. F. and Galizia, C. G. (2007). Processing of odor mixtures in the Drosophila antennal lobe reveals both global inhibition and glomerulus-specific interactions. *J. Neurosci.* **27**, 11966-11977.

Simon, A. F., Daniels, R., Romero-Calderón, R., Grygoruk, A., Chang, H.-Y., Najibi, R., Shamouelian, D., Salazar, E., Solomon, M., Ackerson, L. C. et al. (2008). *Drosophila* vesicular monoamine transporter mutants can adapt to reduced or eliminated vesicular stores of dopamine and serotonin. *Genetics* **181**, 525-541.

Sinakevitch, I. and Strausfeld, N. J. (2004). Chemical neuroanatomy of the fly's movement detection pathway. *J. Comp. Neurol.* **468**, 6-23.

Sinakevitch, I., Douglass, J. K., Scholtz, G., Loesel, R. and Strausfeld, N. J. (2003). Conserved and convergent organization in the optic lobes of insects and isopods, with reference to other crustacean taxa. *J. Comp. Neurol.* **467**, 150-172.

Strambi, C., Cayre, M., Sattelle, D. B., Augier, R., Charpin, P. and Strambi, A. (1998). Immunocytochemical mapping of an RDL-like GABA receptor subunit and of GABA in brain structures related to learning and memory in the cricket *Acheta domesticus*. *Learn. Mem.* **5**, 78-89.

Strausfeld, N. J., Kong, A., Milde, J. J., Gilbert, C. and Ramaiah, L. (1995). Oculomotor control in calliphorid flies: GABAergic organization in heterolateral inhibitory pathways. *J. Comp. Neurol.* **361**, 298-320.

Su, H. and O'Dowd, D. K. (2003). Fast synaptic currents in Drosophila mushroom body Kenyon cells are mediated by alpha-bungarotoxin-sensitive nicotinic acetylcholine receptors and picrotoxin-sensitive GABA receptors. *J. Neurosci.* **23**, 9246-9253.

Sun, B.-C. and Salvaterra, P. (1995). Two Drosophila nervous system antigens, Nervana 1 and 2, are homologous to the beta subunit of Na^+,K(+)-ATPase. *Proc. Natl. Acad. Sci. USA* **92**, 5396-5400.

Takemura, S. Y., Lu, Z. and Meinertzhagen, I. A. (2008). Synaptic circuits of the Drosophila optic lobe: the input terminals to the medulla. *J. Comp. Neurol.* **509**, 493-513.

van de Goor, J., Ramaswami, M. and Kelly, R. (1995). Redistribution of synaptic vesicles and their proteins in temperature-sensitive shibire(ts1) mutant Drosophila. *Proc. Natl. Acad. Sci. USA* **92**, 5739-5743.

Wagh, D. A., Rasse, T. M., Asan, E., Hofbauer, A., Schwenkert, I., Durrbeck, H., Buchner, S., Dabauvalle, M.-C., Schmidt, M. and Qin, G. (2006). Bruchpilot, a protein with homology to ELKS/CAST, is required for structural integrity and function of synaptic active zones in drosophila. *Neuron* **49**, 833-844.

Warzecha, A. K., Egelhaaf, M. and Borst, A. (1993). Neural circuit tuning fly visual interneurons to motion of small objects. I. Dissection of the circuit by pharmacological and photoinactivation techniques. *J. Neurophysiol.* **69**, 329-339.

Wilson, R. I. and Laurent, G. (2005). Role of GABAergic inhibition in shaping odor-evoked spatiotemporal patterns in the Drosophila antennal lobe. *J. Neurosci.* **25**, 9069-9079.

Wojcik, S. M., Katsurabayashi, S., Guillemin, I., Friauf, E., Rosenmund, C., Brose, N. and Rhee, J. S. (2006). A shared vesicular carrier allows synaptic corelease of GABA and glycine. *Neuron* **50**, 575-587.

Yasuyama, K., Meinertzhagen, I. A. and Schurmann, F. W. (2002). Synaptic organization of the mushroom body calyx in *Drosophila melanogaster*. *J. Comp. Neurol.* **445**, 211-226.

Zhu, Y., Nern, A., Zipursky, S. L. and Frye, M. A. (2009). Peripheral visual circuits functionally segregate motion and phototaxis behaviors in the fly. *Curr. Biol.* **19**, 613-619.

Zinsmaier, K. E., Hofbauer, A., Heimbeck, G., Pflugfelder, G. O., Buchner, S. and Buchner, E. (1990). A cysteine-string protein is expressed in retina and brain of Drosophila. *J. Neurogenet.* **7**, 15-29.